https://doi.org/10.48048/tis.2024.7193

Input Shaping for Flexible Systems with Non-Zero Initial Conditions

Ittidej Moonmanngmee*, Pachara Juyploy and Withit Chatlatanagulchai

Control of Robot and Vibration Laboratory, Department of Mechanical Engineering, Faculty of Engineering, Kasetsart University, Bangkok 10900, Thailand

(*Corresponding author's e-mail: ittidej.m@ku.th)

Received: 9 June 2023, Revised: 19 July 2023, Accepted: 21 July 2023, Published: 20 September 2023

Abstract

Input shaping is a finite-impulse response (FIR) filter whose coefficients are designed to produce a shaped input that avoids exciting lightly-damped modes. As a result, flexible systems can be commanded to move quickly from point to point with minimum residual vibration. However, traditional input shaping techniques assume zero initial conditions, limiting their usability for systems with non-zero initial conditions, such as, emergency stops of cranes. Besides, in practice, movement of flexible systems is often initiated when the systems are not completely stationary. In these situations, the performance of the input shaping technique deteriorates. In this paper, a modification of shaper's impulse sequence at the beginning of the move is proposed to bring the moving flexible system to a stop before commencing movement. The modification utilizes the work and energy method to determine the distance and time as functions of the initial states for base excitation of flexible systems, rendering its application to nonlinear systems. By concatenating this modification with the existing input shapers, a novel shaper called the non-zero initial conditions zero-vibration-derivative (NI-ZVD^k) input shaper is introduced. The NI-ZVD^k input shaper effectively prevents the movement of flexible systems from their initial states. To demonstrate the effectiveness of the approach, a 2-mass system is utilized as a benchmark for general flexible systems with 2 degrees of freedom. Various types of motion, including pure translation, pure rotation, and combined translation-rotation, are considered. Extensive simulation results showed that, using the proposed NI-ZVD^k input shaper, the flexible systems can move from non-zero initial conditions to their desired destinations with less time and less residual vibration.

Keywords: Vibration control, Input shaping, Residual vibrations, Non-zero initial conditions, Nonlinear vibratory systems, Flexible systems, Work and energy method

Introduction

Input shaping is a simple yet effective technique to reduce residual vibration in point-to-point movement of flexible systems. Its applications are expanding from crane [15,19,22,24,40], hard disk drive [28], industrial robot manipulator [20,21,35], liquid sloshing [1], flexible spacecraft [27,42], X-Y platform [33,39,41], elevator [14], quadrotor and drone [5,12,18], DC motor, car wiper [28], offshore structure [36], to micro and nano systems like nano positioner and MEMS actuator [2].

The original idea of input shaping was proposed by Smith in [31], under the name *Posicast*. **Figure 1** illustrates the Posicast idea. The objective is to move the trolley and the pendulum from position 1 to 2 without residual oscillation at position 2. **Figure 1(a)** is the initial resting state. In **Figure 1(b)**, a force moves the trolley to midway between positions 1 and 2, causing the pendulum to swing from position 1 to position 2, as shown in **Figure 1(c)**. Then, the trolley is immediately moved to position 2 so that the pendulum stays at position 2 without residual oscillation as in **Figure 1(d)**. Singer and Seering [30], extended the Posicast control by increasing its robustness to parameter uncertainty and patented the technique under the name *input shaping.*

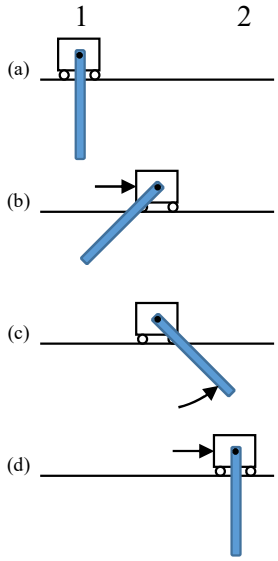

Figure 1 An application of half-cycle Posicast.

The Posicast control as well as the input shaping technique assume that the flexible system has zero initial conditions, that is, zero position and zero velocity. If the system has non-zero initial conditions, the techniques will not suppress the residual vibration. In some cases, the input technique even amplifies the residual vibration. To design an input shaper that can function well despite the presence of non-zero initial conditions is important because of 2 reasons. First, in practice, when the flexible system is moved from point to point, it is rarely stop completely. Then, the next movement has to start from non-zero initial conditions, which almost always degrades the vibration suppression performance. Second, some application such as emergency stop of a crane requires the flexible system to stop from non-zero initial conditions.

Existing literature that discusses the problem with non-zero initial conditions and proposes a way to remedy is very rare. Veciana *et al.* [37], showed that the non-zero initial conditions are equivalent to the plant-input disturbance. The plant-input disturbance produced an impulse response whose unknown parameter could be found on-line. This impulse response was added to the response of a pulse reference signal, which had been passed through an input shaper. The total response equaled the residual vibration, which was set equal to zero to find the time locations and amplitudes of the impulses in the input shaper. However, the technique was valid only for the pre-selected unshaped command, and the technique did not have the filter functionality of an input shaper. Dhanda *et al.* [9], included the effect of the non-zero initial conditions directly in the residual vibration constraint. An optimal shaping filter was found from 2 optimization problems. The first optimization problem was to find coefficients of the optimal shaping filter. The general solution turned out to produce a bang-bang signal. The second optimization problem was to find the switching times of the bang-bang signal. This optimization problem was a nonlinear parametric optimization problem, which could only be performed off-line. Therefore, this technique was not suitable for on-line implementation where the amount of the initial conditions could not be pre-specified.

Hong and Hong [15], used 2 stages of input shaping and nonlinear control for crane under simultaneous hoisting and transverse motion. They mentioned a necessity to account for non-zero initial conditions during the start of the transverse motion; however, they did not provide solution to this problem. Huey *et al.* [17], proposed the closed-loop signal shaping where the input shaper was placed inside the feedback loop. The closed-loop signal shaping could not reduce vibration from the plant-input disturbance or from the non-zero initial conditions. However, they mentioned the outside-the-loop input shaping where the input shaper was placed outside the feedback loop. The outside-the-loop input shaping relied on the feedback controller to reduce vibrations from disturbances, non-zero initial conditions, and nonlinearities. Chatlatanagulchai and Benjalersyarnon [3], and Chatlatanagulchai and Kijdech [4], considered the outside-the-loop input shaping. The quantitative feedback controller, detailed by Horowitz [16], was used to reduce vibration from non-zero initial conditions. However, the technique had to rely on the feedback controller. Pereira *et al.* [26], applied the algebraic identification technique, proposed by Fliess and Sira-Ramirez [13], to indirect adaptive input shaping of a second-order flexible system. The algebraic identification technique

was used to identify ω_n and ζ in real time for the input shaper. The algebraic identification technique found second-order derivatives of the Laplace transform equation of the system's equation of motion. As a result, the technique did not depend on the initial conditions. However, only the identification of the mode parameters was not affected by the initial conditions, not the input shaping.

Recent literature addressing the issue of non-zero initial conditions still primarily focuses on linear systems. These studies incorporate the effect of non-zero initial conditions directly into the residual vibration constraint. Dhanda *et al.* [10], and Newman *et al.* [25], proposed pole-zero cancellation techniques to address flexible modes and considered the effect of initial states in the sensitivity function. The impulse sequences of the zero-vibration (ZV), zero-vibration-derivative (ZVD), and specified intensity (SI) shapers were designed to include terms that accounted for non-zero initial conditions. The solution to the time-optimal problem was found to be a bang-bang signal [10]. Newman *et al.* [24], addressed the problem of non-zero initial conditions in the phase-plane vector diagram. The initial conditions of an underdamped system are calculated and represented by an impulse with magnitude and phase. The initial vibration is canceled by adding a sum of 2 impulses that act as opposing vectors, directly countering the initial impulse. Wahrburg *et al.* [38], proposed a 2-pulse input shaper for systems with non-zero initial conditions and a large class of input signals. The proposed shaper re-parameterization based on the initial conditions and the input signal is computationally slim such that it can be performed on-line. However, it should be noted that the shaper designed for non-zero initial conditions was limited to linear underdamped systems and could not be applied to nonlinear systems.

In this paper, a modification to the ordinary input shaping is proposed to obtain zero initial conditions prior to applying the traditional zero-vibration and k-derivative (ZVD^k) input shaping. **Figure 2** illustrates the idea. In **Figure 2(a)**, the cart is at position 1 whereas the pendulum is moving toward the cart. In **Figure 2(b)**, the cart moves to the left by a pre-computed distance. In **Figure 2(c)**, the pendulum swings past the cart and stops at position 1. In **Figure 2(d)**, the cart moves back to the right; both the cart and pendulum are at the original position 1 with zero initial conditions. The 2 unknown parameters are the moving distance of the cart and the time the cart moves back to the original position. Both parameters can be found from the work and energy method.

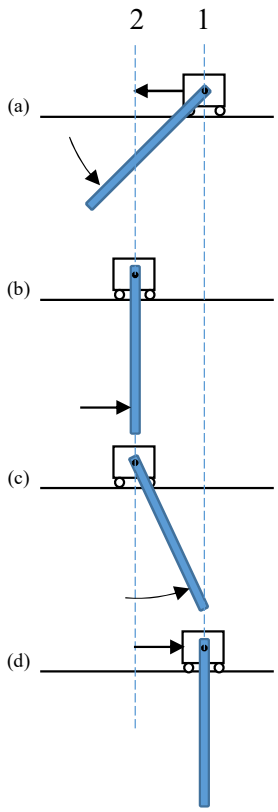

Figure 2 The proposed idea to obtain zero initial conditions.

In the existing input shaping literature, the work and energy method was mainly used for input shaping for nonlinear systems by few researchers. Kozak [21], and Smith *et al.* [32], applied the conservation of energy principle in designing nonlinear input shaper for configuration dependent nonlinear systems. They considered 2 cases: Base excitation and force excitation. In the base excitation case, a ZV input shaper was designed to shape the profile of the base to move the mass from 1 resting point to another resting point without residual vibration. The amplitudes and time locations of the input shaper's impulses were solved from the work and energy equation from moving the mass from point to point. In the force excitation case, a ZV input shaper was designed to shape the profile of the input force to move the mass from a resting point to another resting point without residual vibration. Again, the input shaper was designed from the work and energy equation. References [6,7], by Chen *et al.* considered a mass-spring system with Duffing nonlinear spring stiffness. A shaped force was designed to bring the mass from rest to rest without residual vibration. To achieve that, a force was found from the work and energy principle to bring the mass from rest to rest. Then, another force was found from the force and acceleration principle to stop the mass from vibrating. Do *et al.* [11], derived a closed-form energy-based shaped input voltage to eliminate bouncing in a micro-electro-mechanical-system (MEMS) contact switch having electrostatic actuation. The time locations of the 2 actuation voltage pulses were found from the work and energy principle in order to bring the switch to its destination with zero velocity.

This paper proposes an idea to achieve zero initial conditions, as shown in **Figure 2**. The work and energy principle was employed to determine the moving distance of the cart and the time required for the cart to return to its original position. This modification effectively prevents non-zero initial conditions at the beginning of the movement and can be combined with the traditional ZVD^k shaper by concatenating the impulse sequences. The technique was applied to 3 distinctive systems which are the 2-mass system (translational system), the flexible-joint robot manipulator (rotational system), and the cart-pendulum system (translational and rotational system). For the 2-mass system, a simulation showed that the proposed idea could stop the mass from non-zero initial conditions. For the flexible-joint robot, a non-zero initial conditions ZVD^k (NI-ZVD^k) input shaper was proposed. Simulations showed that the NI-ZVD^k shaper, when compared with the ZVD^k shaper, could effectively suppress residual vibration of the flexible-joint robot with non-zero initial conditions. For the cart-pendulum system, a nonlinear plant model was used as the truth model in the simulation. Therefore, the ZVD^5 shaper was used to provide enough robustness. In simulation, the NI-ZVD^5 shaper could suppress the residual vibration of the pendulum effectively when compared to the ZVD^5 shaper. The cart-pendulum system can move from non-zero initial conditions to its destination with significantly less settling time and residual vibration.

The proposed technique offers several advantages over previously proposed work as follows:

1) Suppress residual vibration from non-zero initial conditions. Typical input shapers cannot handle vibration from non-zero initial conditions. In some cases, the input shapers may even cause more residual vibration in the system.

2) Proposed NI-ZVD^k shaper is a filter. Being a filter, it can be redesigned on-line and can work with arbitrary amount of non-zero initial conditions.

3) Design parameters are found in closed form. For undamped or lightly damped systems, the parameters of the NI-ZVD^k shaper are in closed form. The technique does not require a large amount of computation resource as those using the optimization problem.

4) Does not require feedback control. NI-ZVD^k can be implemented as a standalone filter with or without the presence of feedback control.

5) Applicable to nonlinear systems. Because the modification was designed using the work and energy principle, it is applicable to nonlinear systems when concatenated with a nonlinear input shaper.

6) Simplicity and versatility. The NI-ZVD^k is just a normal ZVD^k shaper with 2 additional impulses at the beginning of the impulse sequence to stop the movement from non-zero initial conditions before the normal input shaping can begin. It is designed from a simple idea without complicated algorithm. Other input shapers can also replace the ZVD^k shaper, providing better performance.

The paper is organized in the following order. Section 2 illustrates the proposed idea with the 2-mass system via simulation. Section 3 contains simulations of a flexible-joint robot manipulator. The NI-ZVD^k shaper is compared with the normal ZVD^k shaper. Section 4 presents simulation results of the cart-pendulum system. Section 5 is discussions and conclusions.

The paper is organized in the following order. Section 2 illustrates the proposed idea with the 2-mass system as a benchmark. A modification to prevent non-zero initial conditions concatenating with the traditional ZVD^k shaper is presented in Section 3 for the flexible-joint robot manipulator, and Section 4 the cart-pendulum system. Simulation results comparing the NI-ZVD^k shaper with the normal ZVD^k shaper. Section 5 is conclusions.

Two-mass system

Consider the 2-mass system shown in **Figure 3**, consisting of 2 entities connected by a flexible element and dampers. In general, this system encompasses a large majority of translational motion of actual rigid-flexible systems. The driving mass m_1 represents the rigid part and the driven mass m_2 the flexible part, corresponding to the absolute positions x_1 and x_2, respectively. The parameters k, c_0, c are the spring stiffness and 2 damping constants, while f is the control force.

The objective is to move both masses from the origin to a displacement X with zero residual vibrations and in a shortest time possible T, that is;

$$\left.\begin{Bmatrix} x_1 \\ x_2 \end{Bmatrix}\right|_{t=T} = \begin{Bmatrix} X \\ X \end{Bmatrix}, \left.\begin{Bmatrix} \dot{x}_1 \\ \dot{x}_2 \end{Bmatrix}\right|_{t=T} = \begin{Bmatrix} 0 \\ 0 \end{Bmatrix}. \tag{1}$$

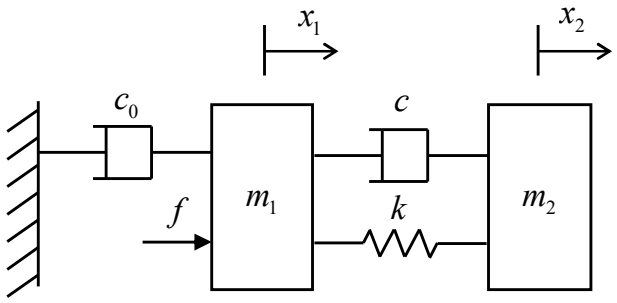

Figure 3 Two-mass system.

Suppose there are non-zero initial conditions at the mass m_2 that is;

$$\left.\begin{Bmatrix} x_1 \\ x_2 \end{Bmatrix}\right|_{t=0} = \begin{Bmatrix} 0 \\ x_{20} \end{Bmatrix}, \left.\begin{Bmatrix} \dot{x}_1 \\ \dot{x}_2 \end{Bmatrix}\right|_{t=0} = \begin{Bmatrix} 0 \\ \dot{x}_{20} \end{Bmatrix}.$$

A modification is proposed in this paper to bring the mass m_2 to a stop before the system commences its movement as usual. By this way, the performance of the input shaping technique will not be degraded by the non-zero initial conditions.

Consider the general scenario shown in **Figure 4**. The coordinates x_1 and x_2 are measured from equilibrium positions, where the spring k and the damper c are unstretched. In **Figure 4(a)**, the mass m_2 has an initial position of x_{20} and initial velocity of $\dot{x}_{20}$ and is moving toward the mass m_1. In **Figure 4(b)**, the mass m_1 moves to the right by a distance A_0. The distance A_0 was pre-computed so that the mass m_2 will rest at the origin $x_2 = 0$. In **Figure 4(c)**, the mass m_2 reaches the point $x_2 = A_0$ where the spring and damper change from stretch to compress. At this position, the mass m_2 has a velocity $\dot{x}_{21}$. In **Figure 4(d)**, the mass m_1 moves back to the origin $x_1 = 0$ when the mass m_2 reaches the origin $x_2 = 0$ with zero velocity. In **Figure 4(e)**, both masses m_1 and m_2 are back at their origins with zero velocities. The normal input shaping technique can then be used to move both masses to a displacement X with zero residual vibrations as stated in Eq. (1).

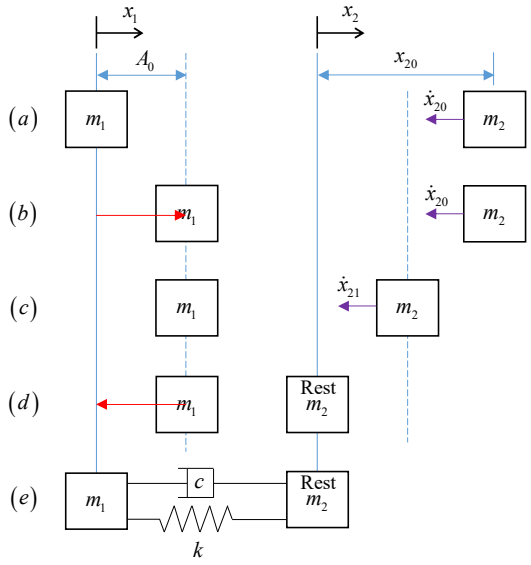

Figure 4 Diagram of a 2-mass system when the mass m_2 has non-zero initial conditions.

The distance A_0 and the time the mass m_1 moves back to the origin $x_1 = 0$ can be calculated using the work and energy principle. Let t_{01} and t_{02} be the time the mass m_1 moves to the point $x_1 = A_0$ and moves back to the origin $x_1 = 0$, respectively.

Undamped system

For simplicity of exposition, undamped case where $c = 0$ is first considered. The distance A_0 can be computed from applying the work and energy principle to the mass m_2, moving from **Figures 4(b) - 4(d)**. From the work and energy principle;

$$\begin{aligned} &U_{b\to d} = T_d - T_b \\ &\left[\frac{1}{2}k\left(x_{20} - A_0\right)^2\right] + \left(-\frac{1}{2}kA_0^2\right) = 0 - \frac{1}{2}m_2\dot{x}_{20}^2, \end{aligned} \tag{2}$$

where $U_{b\to d}$ is the work by the spring force to move the mass m_2 from (b) to (d) and T_d and T_b are the kinetic energy of the mass m_2 at point (d) and (b), respectively. The distance A_0 is then given by;

$$A_0 = \frac{\left(\frac{1}{2}kx_{20}^2 + \frac{1}{2}m_2\dot{x}_{20}^2\right)}{kx_{20}}. \tag{3}$$

To find the time t_{02} the work and energy principle can then again be applied to the movement of the mass m_2 from point (b) to a general point x_2, yielding;

$$\begin{aligned} &U_{b\to x_2} = T_{x_2} - T_b \\ &\left[\frac{1}{2}k\left(x_{20} - A_0\right)^2\right] + \left[-\frac{1}{2}k\left(A_0 - x_2\right)^2\right] = \frac{1}{2}m_2\dot{x}_2^2 - \frac{1}{2}m_2\dot{x}_{20}^2. \end{aligned} \tag{4}$$

The general velocity $\dot{x}_2$ of the mass m_2 can then be solved as;

$$\dot{x}_2 = \sqrt{\frac{k\left(x_{20} - A_0\right)^2 - k\left(A_0 - x_2\right)^2 + m_2\dot{x}_{20}^2}{m_2}}.$$

Then, the time t_{02} can be found from;

$$t_{02} = \int_{x_{20}}^{0} \frac{1}{\dot{x}_2} dx_2, \tag{5}$$

which is the time the mass m_2 reaches the point $x_2 = 0$.

To demonstrate the effectiveness of the proposed technique, simulation was performed with the 2-mass system in **Figure 3**. The plant parameters are $m_1 = 2$ kg, $m_2 = 3$ kg, $c = 0$ kg-s^{-1}, $c_0 = 30$ kg-s^{-1}, and $k = 1$ kg-s^{-2}. The plant model is given by;

$$\dot{x} = \begin{bmatrix} 0 & 1 & 0 & 0 \\ -\frac{k}{m_1} & -\frac{(c+c_0)}{m_1} & \frac{k}{m_1} & \frac{c}{m_1} \\ 0 & 0 & 0 & 1 \\ \frac{k}{m_2} & \frac{c}{m_2} & -\frac{k}{m_2} & -\frac{c}{m_2} \end{bmatrix} x + \begin{Bmatrix} 0 \\ \frac{1}{m_1} \\ 0 \\ 0 \end{Bmatrix} f,$$

$$y = \begin{bmatrix} 1 & 0 & 0 & 0 \end{bmatrix} x,$$

where $x = \left[x_1, \dot{x}_1, x_2, \dot{x}_2\right]^T$ is the state vector and the plant output $y = x_1$ is the position of the mass m_1. A proportional controller with a gain $k_P = 100$ was used to make the output track a pulse reference r, which is a unit-step signal convoluting with a sequence of impulses;

$$\begin{bmatrix} A_i \\ t_i \end{bmatrix} = \begin{bmatrix} A_0 & -A_0 \\ 0 & t_{20} \end{bmatrix}, \tag{6}$$

where A_i are the impulse amplitudes and t_i are the impulse time locations.

Figure 5(a) contains simulation result without the proposed technique. The mass m_1 was merely regulated at the origin $x_1 = 0$. The mass m_2 was given an initial position of $x_{20} = 1$ m and an initial velocity of $\dot{x}_{20} = -0.1$ m/s. It can be seen that the mass m_2 oscillates perpetually with an amplitude of 1 m. **Figure 5(b)** contains simulation result with the proposed technique implemented. The amplitude A_0 for the mass m_1 to move in order to suppress the vibration of the mass m_2 was computed according to Eq. (3) and the time t_{02} for the mass m_1 to move back to the origin $x_1 = 0$ was computed according to Eq. (5). A_0 is 0.52 m and t_{02} is 4.4 s. The shaped reference signal r is then a pulse of the amplitude 0.515 m and width 4.4 s, shown as dotted line in **Figure 5(b)**. The output $y = x_1$ was commanded by the proportional controller to follow the pulse reference input closely. Vibration of the mass m_2 was suppressed to a steady-state amplitude of 0.054 m, which is 5.4 % of the case when the proposed modification was not implemented. Note that the vibration was not completely suppressed because the output y did not follow the desired reference r perfectly.

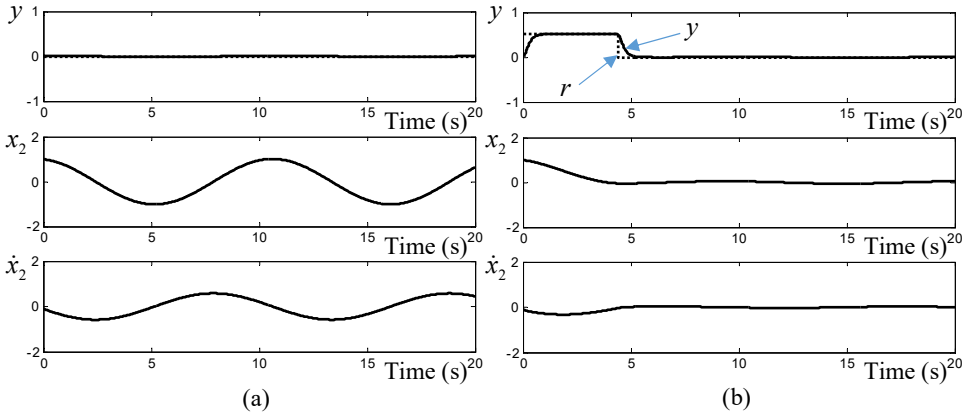

Figure 5 Simulation of the undamped 2-mass system. (a) Without the proposed technique. (b) With the proposed technique.

Damped system

If the 2-mass system in **Figure 3** has a viscous damper, that is, $c > 0$, the work done by the viscous damper must be included in the work and energy equations. Eq. (2) becomes;

$$\left[\frac{1}{2}k\left(x_{20}-A_0\right)^2\right]+\left(-\frac{1}{2}kA_0^2\right)-\int_{x_{20}}^{0}c\dot{x}_2dx_2=0-\frac{1}{2}m_2\dot{x}_{20}^2, \tag{7}$$

and Eq. (4) becomes;

$$\left[\frac{1}{2}k\left(x_{20}-A_0\right)^2\right]+\left[-\frac{1}{2}k\left(A_0-x_2\right)^2\right]-\int_{x_{20}}^{x_2}c\dot{x}_2dx_2=\frac{1}{2}m_2\dot{x}_2^2-\frac{1}{2}m_2\dot{x}_{20}^2. \tag{8}$$

Eq. (8) can be used to find $\dot{x}_2$; then, Eq. (7) can be used to compute A_0. Eq. (5) can again be used to find the time t_{02}.

The proposed 2-mass system presented in this section was used as a benchmark, with m_1 considered as the rigid part excited by its position, while m_2 as the flexible part. With this configuration, it can be extended to other general rigid-flexible systems with 2-degrees-of-freedom, depending on the motion type of each part (translation or rotation). In Sections 3 and 4, 2 case studies, namely the flexible-joint robot manipulator and the cart-pendulum system, will be utilized to demonstrate their applications in both rotational and translational-rotational systems.

Case study 1: Flexible-joint robot manipulator

A flexible-joint robot manipulator is a robotic system composed of multiple interconnected links, where the joints possess varying degrees of flexibility. It has been utilized in a wide range of application areas, including manufacturing/assembly, industrial automation, medical, aerospace, etc. In this paper, a simple model of a 2-degrees-of-freedom flexible-joint robot manipulator was considered. The top view is shown in **Figure 6**, where θ_1 and θ_2 are the absolute angular position of the link and motor hub, respectively. The parameters $\alpha, \beta, L_1, L_2, r_1, r_2,$ and r_3 are related dimensions. Note that when the link is in neutral position, that is, $\theta_1 = \theta_2$, the 2 springs are unstretched.

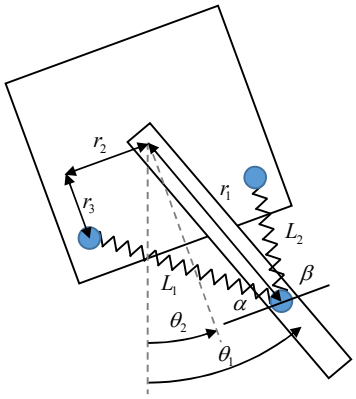

Figure 6 Top-view diagram of the flexible-joint robot.

Nonlinear system model

Using the Euler-Lagrange method, the nonlinear equations of motion of the system are given by;

$$\begin{bmatrix} J_l + J_p & 0 \\ 0 & J_h \end{bmatrix}\begin{bmatrix} \ddot{\theta}_1 \\ \ddot{\theta}_2 \end{bmatrix} + \begin{bmatrix} c_1 & -c_1 \\ -c_1 & c_1 + c_2 \end{bmatrix}\begin{bmatrix} \dot{\theta}_1 \\ \dot{\theta}_2 \end{bmatrix} + \begin{bmatrix} -M_k \\ M_k \end{bmatrix} = \begin{bmatrix} 0 \\ T \end{bmatrix}, \tag{9}$$

where M_k is the moment of the nonlinear spring, which is given by;

$$\begin{aligned} M_k &= -k_s\left(L_1 - L\right)\left(\cos\alpha\right)r_1\cos\left(\theta_1 - \theta_2\right) + k_s\left(L_1 - L\right)\left(\sin\alpha\right)r_1\sin\left(\theta_1 - \theta_2\right) \\ &\quad + k_s\left(L_2 - L\right)\left(\cos\beta\right)r_1\cos\left(\theta_1 - \theta_2\right) + k_s\left(L_2 - L\right)\left(\sin\beta\right)r_1\sin\left(\theta_1 - \theta_2\right), \\ L_1 &= \sqrt{\left(r_1\cos\left(\theta_1 - \theta_2\right) - r_3\right)^2 + \left(r_1\sin\left(\theta_1 - \theta_2\right) + r_2\right)^2}, \\ L_2 &= \sqrt{\left(r_1\cos\left(\theta_1 - \theta_2\right) - r_3\right)^2 + \left(-r_1\sin\left(\theta_1 - \theta_2\right) + r_2\right)^2}, \\ \alpha &= \tan^{-1}\left(\frac{r_1\cos\left(\theta_1 - \theta_2\right) - r_3}{r_1\sin\left(\theta_1 - \theta_2\right) + r_2}\right),\ \beta = \tan^{-1}\left(\frac{r_1\cos\left(\theta_1 - \theta_2\right) - r_3}{-r_1\sin\left(\theta_1 - \theta_2\right) + r_2}\right), \end{aligned}$$

and T is the motor torque. Parameter values of the flexible-joint robot as well as their descriptions are given in **Table 1**.

Table 1 Parameter values of the flexible-joint robot.

Parameter	Description	Values
l, r_1, r_2, r_3, L	Link length, dimensions r_1, r_2, r_3 in Error! Reference source not found., unstretched spring length	0.3, 0.1, 0.05, 0.04, 0.078 m
m_l, m_p	Link mass, payload mass	0.05, 0.1 kg
J_l, J_h, J_p	Link, hub, and payload masses moment of inertia about pivot point	0.0015, 0.0011, 0.0281 kg-m^2
c_1, c_2	Damping constant at link bearing, damping constant at motor bearing	0.1, 1 kg-s^{-1}
k_s	Spring constant	1,000 kg-s^{-2}

Linearized system model

The nonlinear equations of motion Eq. (9) can be linearized about $\theta_1 - \theta_2 = 0$ as;

$$\begin{bmatrix} \dot{x}_1 \\ \dot{x}_2 \\ \dot{x}_3 \\ \dot{x}_4 \end{bmatrix} = \begin{bmatrix} 0 & 1 & 0 & 0 \\ -\dfrac{k_{slin}}{J_l + J_p} & -\dfrac{c_1}{J_l + J_p} & \dfrac{k_{slin}}{J_l + J_p} & \dfrac{c_1}{J_l + J_p} \\ 0 & 0 & 0 & 1 \\ \dfrac{k_{slin}}{J_h} & \dfrac{c_1}{J_h} & -\dfrac{k_{slin}}{J_h} & -\left(\dfrac{c_2}{J_h} + \dfrac{c_1}{J_h}\right) \end{bmatrix} \begin{bmatrix} x_1 \\ x_2 \\ x_3 \\ x_4 \end{bmatrix} + \begin{bmatrix} 0 \\ 0 \\ 0 \\ \dfrac{1}{J_h} \end{bmatrix} T, \tag{10}$$

where $x_1 = \theta_1$, $x_2 = \dot{\theta}_1$, $x_3 = \theta_2$, $x_4 = \dot{\theta}_2$, and $k_{slin} = \left.\dfrac{\partial M_k}{\partial(\theta_1 - \theta_2)}\right|_{\theta_1 - \theta_2 = 0} = 8.2$ kg-s^{-2} is the linearized spring constant.

Initial movement

First, consider the undamped system, that is, $c_1 = 0$. Following the proposed technique from the previous section, the initial movement amplitude A_0 can be found from applying the work and energy principle to the link, moving from **Figures 4(b) - 4(d)**. From the work and energy principle;

$$\begin{aligned} &U_{b\to d} = T_d - T_b \\ &\left[\frac{1}{2}k_{slin}\left(\theta_{10} - A_0\right)^2\right] + \left(-\frac{1}{2}k_{slin}A_0^2\right) = 0 - \frac{1}{2}\left(J_l + J_p\right)\dot{\theta}_{10}^2. \end{aligned} \tag{11}$$

Note that the motor hub angular position θ_2 is analogous to x_1 of the 2-mass system, and the link angular position θ_1 is analogous to x_2 of the 2-mass system. By solving Eq. (11), the initial movement amplitude A_0 is then given by;

$$A_0 = \frac{\left[\frac{1}{2}k_{slin}\theta_{10}^2 + \frac{1}{2}\left(J_l + J_p\right)\dot{\theta}_{10}^2\right]}{k_{slin}\theta_{10}}. \tag{12}$$

The time t_{02} can be found from applying the work and energy principle to the movement of the link from point (b) to a general point θ_1, resulting in;

$$\begin{aligned} &U_{b\to\theta_1} = T_{\theta_1} - T_b \\ &\left[\frac{1}{2}k_{slin}\left(\theta_{10} - A_0\right)^2\right] + \left[-\frac{1}{2}k_{slin}\left(A_0 - \theta_1\right)^2\right] = \frac{1}{2}\left(J_l + J_p\right)\dot{\theta}_1^2 - \frac{1}{2}\left(J_l + J_p\right)\dot{\theta}_{10}^2. \end{aligned} \tag{13}$$

The general velocity $\dot{\theta}_1$ of the link is then solved from Eq. (13), resulting in;

$$\dot{\theta}_1 = \sqrt{\frac{k_{slin}\left(\theta_{10} - A_0\right)^2 - k_{slin}\left(A_0 - \theta_1\right)^2 + \left(J_l + J_p\right)\dot{\theta}_{10}^2}{\left(J_l + J_p\right)}}.$$

The time t_{02} can then be found from;

$$t_{02} = \int_{\theta_{10}}^{0} \frac{1}{\dot{\theta}_1} d\theta_1. \tag{14}$$

For the damped case, the work done by the damper $-\int_{\theta_{10}}^{0} c_1 \dot{\theta}_1 d\theta_1$ can be added to the left-hand side of Eq. (11) and $-\int_{\theta_{10}}^{\theta_1} c_1 \dot{\theta}_1 d\theta_1$ to that of Eq. (13).

Input shaping impulse sequence

In this section, the proposed sequence of impulses Eq. (6) is concatenated with the zero vibration (ZV) input shaper. The purpose of the proposed sequence of impulses Eq. (6) is to suppress vibration due to the initial conditions. The ZV input shaper is used to suppress vibration due to the reference signal.

For the proposed sequence of impulses Eq. (6), with initial conditions $\theta_{10} = 2$ rad and $\dot{\theta}_{10} = 0$ rad/s, can be computed from Eqs. (12) and (14) as $A_0 = 1$ rad and $t_{02} = 0.1834$ s, respectively.

In general, a ZVD^k input shaper, where $k = 0, 1, 2, \ldots$, has the total of $k+2$ impulses in the sequence and is shown to have normalized impulse amplitudes and timings as;

$$A_i = \frac{\binom{k+1}{i-1} K^{i-1}}{\sum_{j=0}^{k+1} \binom{k+1}{j} K^j}, \quad t_i = (i-1)\frac{\pi}{\omega_n \sqrt{1-\zeta^2}}, \quad i = 1, 2, \ldots, k+2, \tag{15}$$

where $K = e^{-\frac{\zeta\pi}{\sqrt{1-\zeta^2}}}$ and $\binom{n}{r} = \frac{n!}{r!(n-r)!}$ is the combinations of n things taken r at a time.

Using a proportional controller gain $k_P = 200$ to control the motor hub position θ_2, the natural frequency and damping ratio of the closed-loop system with the linearized plant Eq. (10), can be calculated as $\omega_n = 16.31$ rad/s, $\zeta = 0.0016$.

For the ZV input shaper, $A_i, i = 1, 2,$ can then be computed from Eq. (15) as $A_1 = 0.5013$ and $A_2 = 0.4987$. $t_i, i = 1, 2,$ are calculated from Eq. (15) as $t_1 = 0$ s and $t_2 = 0.1926$ s.

Concatenating the 2 impulse sequences results in a non-zero initial conditions ZV (NI-ZV) input shaping impulse sequence;

$$\begin{bmatrix} A_i \\ t_i \end{bmatrix}_{2\times 4} = \begin{bmatrix} A_0 & -A_0 & A_1 & A_2 \\ 0 & t_{02} & t_{02}+t_1 & t_{02}+t_2 \end{bmatrix} = \begin{bmatrix} 1 & -1 & 0.5013 & 0.4987 \\ 0 & 0.1834 & 0.1834 & 0.3761 \end{bmatrix} \tag{16}$$

as shown in **Figure 7**. The general non-zero initial conditions ZVD^k (NI-ZVD^k) input shaping impulse sequence can be found in a similar manner to that of the NI-ZV shaper. However, to enhance robustness against mode parameter uncertainty, at the expense of having more impulses in the input shaper sequence and consequently a slower time to reach the final reference position.

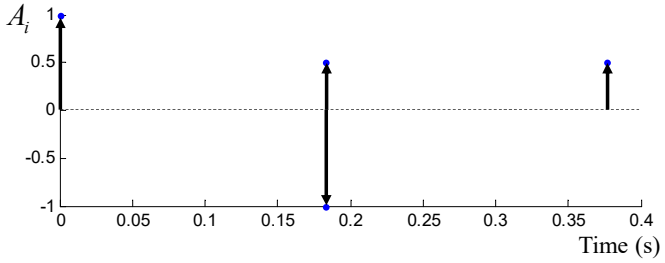

Figure 7 Impulse sequence of the NI-ZV shaper.

Simulation result

The flexible-joint robot has the motor hub position as its output, that is, $y = \theta_2$. The objective is to move the link, whose position is θ_1, to an angle of 1 rad as quickly as possible with minimum residual vibration. With zero initial conditions and perfect model, the ZV shaper should have achieved this objective. However, as can be seen from **Figure 8(a)**, with an initial link angular position $\theta_{10} = 2$ rad, the ZV shaper even amplifies the residual vibration of the link angular position θ_1. This is because the ZV shaper is designed based on an assumption of zero initial conditions. Therefore, it must wait for the system to stop vibrating before the next movement can commence.

With the proposed technique, the ZV input shaping sequence is preceded by a sequence of impulses Eq. (6) that aims to stop the vibration from non-zero initial conditions before the ZV shaper can take effect. **Figure 8(b)** shows the result of applying the NI-ZV impulse sequence Eq. (16) to the robot. The link residual vibration as seen in θ_1 is almost perfectly suppressed by the NI-ZV shaper.

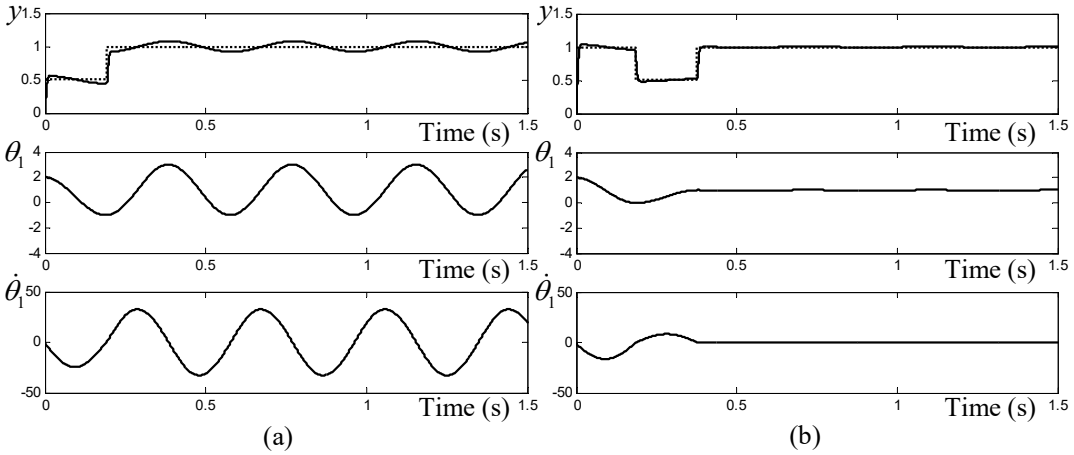

Figure 8 Simulation of the undamped flexible-joint robot. (a) ZV shaper. (b) NI-ZV shaper.

Case study 2: Cart-pendulum system

A cart-pendulum system shown in **Figure 9** is a simple model of a gantry crane, consisting of the cart mass m_C, the link mass m_L, and the payload mass m_P. This system exhibits translational-rotational motion, analogous to the 2-mass system discussed in Section 2, where the entities m_1 and m_2 correspond to m_C and $m_L + m_P$, respectively. Let x_1 and x_2 be the absolute position of the cart and the payload, respectively, θ the relative pendulum angular position, and f the push force to the cart. Descriptions of other plant parameters and their values are given in **Table 2**.

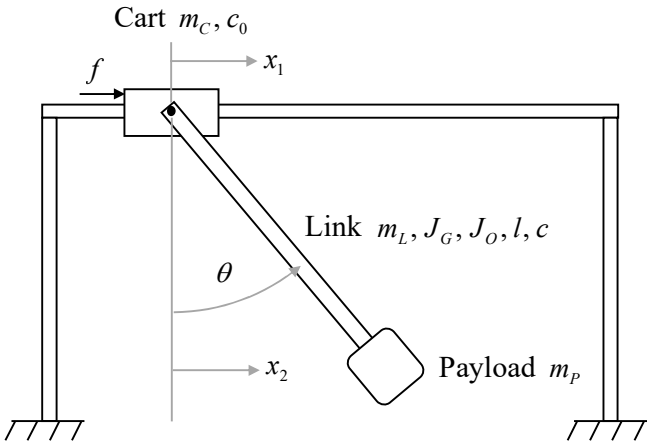

Figure 9 Cart-pendulum system.

Table 2 Descriptions of plant parameters and their values.

Parameter	Description	Values
l	Link length	0.6 m
m_C, m_L, m_P	Cart mass, link mass, payload mass	0.3, 0.2, 0.1 kg
J_G, J_O	Link mass moment of inertia about C.G., link mass moment of inertia about pivot point	0.006, 0.024 kg-m^2
c_0, c	Cart viscous damping constant, link viscous damping constant at pivot point	200 kg-s^{-1}, 0.01 kg-m^2-s^{-1}

Initial movement

Using the diagram in **Figure 4** with the undamped case where $c = 0,$ the work and energy principle, applied to the pendulum, moving from **Figures 4(b) - 4(d)**, gives;

$$\begin{aligned} &U_{b\to d} = T_d - T_b \\ &m_P g\left[l - l\cos\left(\frac{x_{20}-A_0}{l}\right)\right] + m_L g\left[\frac{l}{2} - \frac{l}{2}\cos\left(\frac{x_{20}-A_0}{l}\right)\right] \\ &\quad + m_P g\left[l\cos\left(\frac{A_0}{l}\right) - l\right] + m_L g\left[\frac{l}{2}\cos\left(\frac{A_0}{l}\right) - \frac{l}{2}\right] = 0 - \left[\frac{1}{2}m_P\dot{x}_{20}^2 + \frac{1}{2}J_O\left(\frac{\dot{x}_{20}}{l}\right)^2\right]. \end{aligned} \tag{17}$$

With known initial conditions x_{20} and $\dot{x}_{20}$, the distance A_0 can be found from the equation above using numerical methods. When the initial velocity $\dot{x}_{20} = 0$, Eq. (17) reduces to;

$$m_P g l\left[\cos\left(\frac{A_0}{l}\right) - \cos\left(\frac{x_{20}-A_0}{l}\right)\right] + m_L g\frac{l}{2}\left[\cos\left(\frac{A_0}{l}\right) - \cos\left(\frac{x_{20}-A_0}{l}\right)\right] = 0,$$

which is satisfied when $A_0 = x_{20}/2.$

To find time t_{02}, applying the work and energy principle to the movement of the pendulum from point (b) to a general point x_2 yields;

$$
\begin{aligned}
&U_{b\to x_2} = T_{x_2} - T_b \\
&m_P g\left[l - l\cos\left(\frac{x_{20}-A_0}{l}\right)\right] + m_L g\left[\frac{l}{2} - \frac{l}{2}\cos\left(\frac{x_{20}-A_0}{l}\right)\right] + m_P g\left[l\cos\left(\frac{A_0-x_2}{l}\right) - l\right] \\
&\quad + m_L g\left[\frac{l}{2}\cos\left(\frac{A_0-x_2}{l}\right) - \frac{l}{2}\right] = \left[\frac{1}{2}m_P\dot{x}_2^2 + \frac{1}{2}J_O\left(\frac{\dot{x}_2}{l}\right)^2\right] - \left[\frac{1}{2}m_P\dot{x}_{20}^2 + \frac{1}{2}J_O\left(\frac{\dot{x}_{20}}{l}\right)^2\right].
\end{aligned} \tag{18}
$$

$\dot{x}_2$ can then be found from the equation above, and the time t_{02} can be found from Eq. (5).

For damped case $(c>0)$, the work of the damper $-\int_{\theta_0}^{0} c\dot{\theta}d\theta$, where θ is the pendulum angle and $\theta_0 = x_{20}/l$ is the initial pendulum angle, can be included in the left-hand side of Eq. (17). The work of the damper $-\int_{\theta_0}^{\theta} c\dot{\theta}d\theta$ can be included in the left-hand side of Eq. (18).

Simulation result

Simulation was performed with the cart-pendulum system, shown in **Figure 9**. Its nonlinear plant model is given by;

$$
\begin{bmatrix} m_{11} & m_{12} \\ m_{21} & m_{22} \end{bmatrix}\begin{bmatrix} \ddot{x}_1 \\ \ddot{\theta} \end{bmatrix} + \begin{bmatrix} c_0 & -\left(0.5m_L l + m_P l\right)\dot{\theta} \\ 0 & c \end{bmatrix}\begin{bmatrix} \dot{x}_1 \\ \dot{\theta} \end{bmatrix} + \begin{bmatrix} 0 \\ \left(m_L + 2m_P\right)g0.5l\sin\theta \end{bmatrix} = \begin{bmatrix} f \\ 0 \end{bmatrix}, \tag{19}
$$

where $m_{11} = m_C + m_L + m_P$, $m_{12} = \left(0.5m_L l + m_P l\right)\cos\theta, m_{21} = \left(m_L + 2m_P\right)0.5l\cos\theta$, and $m_{22} = \left(m_L + 4m_P\right)\left(0.5l\cos\theta\right)^2 + \left(m_L + 4m_P\right)\left(0.5l\sin\theta\right)^2 + J_G$.

The nonlinear plant model was linearized about its equilibrium point. A proportional controller gain $k_p = 2,000$ was used to control the cart position $y = x_1$. With the parameter values in **Table 2**, the natural frequency and damping ratio of the closed-loop system were computed from the linearized model as $\omega_n = 4.43$ rad/s, $\zeta = 0.0027$.

Because the nonlinear plant model Eq. (19) will represent the actual cart-pendulum system in the simulation, the computed mode parameters ω_n, ζ contain uncertainty. ZVD[5] input shaper was found to provide satisfactory robustness and vibration suppression result.

With initial conditions $\theta(0) = 10$ deg (or 0.18 rad) and $\dot{\theta}(0) = 0$, the initial distance A_0 was found from Eq. (17) to be $A_0 = 0.0524$ m, and the time t_{02} was found from Eq. (18) and Eq. (5) to be 0.53 s. The ZVD[5] input shaping impulse sequence was found from Eq. (15). The non-zero initial conditions ZVD[5] (NI-ZVD[5]) input shaping impulse sequence is then given by;

$$
\begin{aligned}
\begin{bmatrix} A_i \\ t_i \end{bmatrix} &= \begin{bmatrix} A_0 & -A_0 & A_1 & A_2 & A_3 & A_4 & A_5 & A_6 & A_7 \\ 0 & t_{02} & t_{02}+t_1 & t_{02}+t_2 & t_{02}+t_3 & t_{02}+t_4 & t_{02}+t_5 & t_{02}+t_6 & t_{02}+t_7 \end{bmatrix} \\
&= \begin{bmatrix} 0.052 & -0.052 & 0.016 & 0.095 & 0.236 & 0.313 & 0.232 & 0.092 & 0.015 \\ 0 & 0.53 & 0.53 & 1.24 & 1.95 & 2.66 & 3.37 & 4.08 & 4.79 \end{bmatrix}
\end{aligned}
$$

as shown in **Figure 10**.

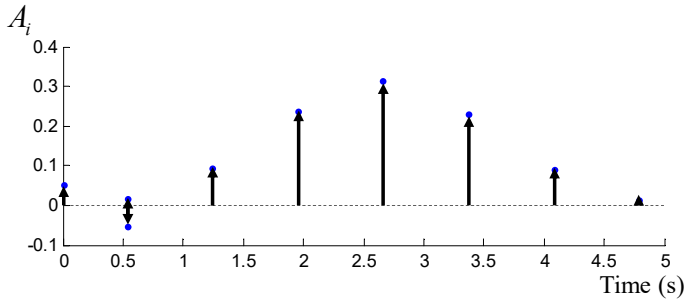

Figure 10 Impulse sequence of the NI-ZVD^5 shaper.

Figure 11 contains the simulation result of the ZVD^5 and NI-ZVD^5 shapers. The initial position of the pendulum was set equal to $\theta(0) = 10$ deg (or 0.18 rad). From **Figure 11(a)**, because the initial position of the pendulum is not zero, the ZVD^5 shaper cannot suppress the residual vibration as can be seen from the pendulum position θ and the payload position x_2. From **Figure 11(b)**, the NI-ZVD^5 shaper can completely suppress the residual vibration because the first 2 impulses A_0 and $-A_0$ in the sequence stops the pendulum movement before the ZVD^5 shaper is applied.

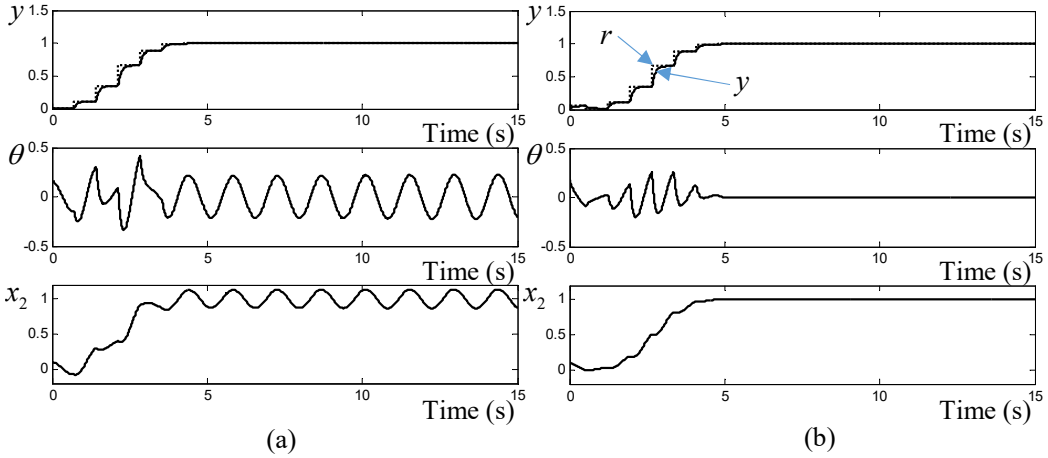

Figure 11 Simulation of the undamped cart-pendulum system. (a) ZVD^5 shaper. (b) NI-ZVD^5 shaper.

Conclusions

This paper considers input shaping of flexible systems when their initial conditions are not zero. Because of the non-zero initial conditions, traditional input shapers cannot properly suppress the residual vibration. This paper proposes a modification at the beginning of the shaper's impulse sequence to stop the flexible system from non-zero initial conditions before the traditional input shaping can begin.

The 2 additional impulses in the impulse sequence are designed based on the work and energy principle. Their objective is to stop the flexible system from moving due to the non-zero initial conditions. The amplitudes and time locations of the 2 impulses are found to be functions of the non-zero initial conditions; therefore, the proposed technique works with arbitrary non-zero initial conditions. Concatenating the 2 additional impulses with traditional ZVD^k input shaper produces non-zero initial conditions ZVD^k (NI-ZVD^k) input shaper. This shaper is a filter that works for arbitrary reference signal under arbitrary non-zero initial conditions.

However, the imperfect elimination of residual vibrations in the systems when they reach the final position arises from 2 reasons: 1) The effectiveness of tracking the designed reference signal from the proposed modification in the shaper's impulse sequence at the beginning depends on the type of controller used. Other controllers can be employed as potential alternatives. 2) For nonlinear plants (such as the

flexible-joint robot manipulator and cart-pendulum system), the computed mode parameters (natural frequency and damping ratio) for designing ZVD^k input shapers contain uncertainty because they were computed from the linearized model. However, this is not a limitation for linear plants (such as the 2-mass system).

Future work is as follows:

1) Evaluate the robustness property
2) Apply to nonlinear input shapers for nonlinear systems
3) Increase the number of impulses to more than two
4) Concatenate with different types of input shapers
5) Extend to multi-input-multi-output systems such as bridge crane

References

[1] A Alshaya and K Kuwait. Command shaping control of a multi-mode flexible system. *In*: Proceedings of the 8th International Conference on Control, Decision and Information Technologies, Istanbul, Turkey. 2022, p. 206-11.

[2] H Ameura, PL Moal, G Bourbona, C Vuillemin and M Sworowski. Suppressing residual vibrations in comb-drive electrostatic actuators: A command shaping technique adapted to nomadic applications. *Sensor. Actuator. Phys.* 2022; **334**, 113366.

[3] W Chatlatanagulchai and T Benjalersyarnon. Closed-loop input shaping with quantitative feedback controller applied to slewed two-staged pendulum. *Walailak J. Sci. Tech.* 2016; **13**, 595-613.

[4] W Chatlatanagulchai and D Kijdech. Outside-the-loop input shaping with quantitative feedback control for flexible systems having non-zero initial conditions. *In*: Proceedings of the 6th Thai Society of Mechanical Engineers, Cha-Am, Phetchaburi, Thailand. 2015.

[5] T Chen and J Shan. Cooperative transportation of cable-suspended slender payload using two quadrotors. *In*: Proceedings of the IEEE International Conference on Unmanned Systems, Beijing, China. 2019, p. 432-7.

[6] T Chen and J Shan. Fixed-time consensus control of multiagent systems using input shaping. *IEEE Trans. Ind. Electron.* 2019; **66**, 7433-41.

[7] KS Chen, TS Yang and JF Yin. Residual vibration suppression for duffing nonlinear systems with electromagnetical actuation using nonlinear command shaping techniques. *J. Vib. Acoust.* 2006; **128**, 778-89.

[8] KS Chen, TS Yang, KS Ou and JF Yin. Design of command shapers for residual vibration suppression in duffing nonlinear systems. *Mechatronics* 2008; **19**, 184-98.

[9] A Dhanda, J Vaughan and W Singhose. Optimal input shaping filters for non-zero initial states. *In*: Proceedings of the American Control Conference, Missouri. 2009.

[10] A Dhanda, J Vaughan and W Singhose. Vibration reduction using near time-optimal commands for systems with nonzero initial conditions. *J. Dyn. Syst. Meas. Contr.* 2016; **138**, 041006.

[11] C Do, M Lishchynska, M Cychowski, K Delaney and M Hill. Energy-based approach to adaptive pulse shaping for control of RF-MEMS DC-contact switches. *J. Microelectromech. Syst.* 2012; **21**, 1382-91.

[12] D Duan, C Zhang, Z Wang and J Li. Active control for helicopters with slung load by combining ADRC and input shaper technology. *In*: Proceedings of the Chinese Control and Decision Conference, Hefei, China. 2020, p. 5368-73.

[13] M Fliess and H Sira-Ramirez. *Closed-loop parametric identification for continuous-time linear systems via new algebraic techniques*. *In*: H Garnier and L Wang (Eds.). Identification of Continuous-Time Models from Sampled Data. Springer, London, 2008, p. 363-91.

[14] J Fortgang, V Patrangenaru and WE Singhose. Scheduling of input shaping and transient vibration absorbers for high-rise elevators. *In*: Proceedings of the American Control Conference, Minneapolis, Minnesota. 2006, p. 1772-7.

[15] KT Hong and KS Hong. Input shaping and VSC of container cranes. *In*: Proceedings of the IEEE on Control Applications, Taipei, Taiwan. 2004, p. 1570-5.

[16] DM Garcia-Sanz. *Quantitative feedback theory*. *In*: J Baillieul and T Samad (Eds.). Encyclopedia of Systems and Control. Springer, London, 2014.

[17] JR Huey, KL Sorensen and WE Singhose. Useful applications of closed-loop signal shaping controllers. *Contr. Eng. Pract.* 2008; **16**, 836-46.

[18] S Ichikawa, A Castro, N Johnson, H Kojima and W Singhose. Dynamics and command shaping control of quadcopters carrying suspended loads. *IFAC PapersOnLine* 2018; **51**, 84-8.

[19] HI Jaafar, Z Mohamed, MA Shamsudin, NAM Subha, L Ramli and AM Abdullahi. Model reference command shaping for vibration control of multimode flexible systems with application to a double-pendulum overhead crane. *Mech. Syst. Signal Process.* 2019; **115**, 677-95.
[20] J Kim and EA Croft. Preshaping input trajectories of industrial robots for vibration suppression. *Robot. Comput. Integrated Manuf.* 2018; **54**, 35-44.
[21] KC Kozak. 2003, Robust command generation for nonlinear systems. Ph. D. Dissertation. Georgia Institute of Technology, Georgia.
[22] JH Montonen, N Nevaranta, M Niemelä and T Lindh. Comparison of extrainsensitive input shaping and swing-angle-estimation-based slew control approaches for a tower crane. *Appl. Sci.* 2022; **12**, 5945.
[23] D Newman, SW Hong and JE Vaughan. Eliminating nonzero initial states in flexible systems through specified insensitivity input shaping. *In*: Proceedings of the American Control Conference, Wisconsin. 2018, p. 3374-9.
[24] D Newman, SW Hong and JE Vaughan. The design of input shapers which eliminate nonzero initial conditions. *J. Dyn. Syst. Meas. Contr.* 2018; **140**, 101005.
[25] D Newman1, J Vaughan and SW Hong. Eliminating initial oscillation in flexible systems by the pole-zero cancellation input shaping technique. *In*: the 7th International Conference of Asian Society for Precision Engineering and Nanotechnology, Seoul, Korea. 2017.
[26] E Pereira, JR Trapero, IM Diaz and V Feliu. Adaptive input shaping for manoeuvring flexible structures using an algebraic identification technique. *Automatica* 2009; **45**, 1046-51.
[27] PT Pham, QC Nguyen, M Yoon and KS Hong. Vibration control of a nonlinear cantilever beam operating in the 3D space. *Sci. Rep.* 2022; **12**, 13811.
[28] MA Salim, A Saad, C Photong, MZ Zain, AR Bakar, NM Yusof and MZ Akop. Modelling and estimation on vibration and noise level of the dynamic wiper system using input shaping strategy. *Int. J. Nanoelectronics Mater.* 2021; **14**, 311-32.
[29] P Shah. 2020, Joint feedback feedforward data driven control design and input shaping techniques for multi actuator hard disk drives. Ph. D. Dissertation. University of California, Berkeley.
[30] NC Singer and WC Seering. Preshaping command inputs to reduce system vibration. *J. Dyn. Syst. Meas. Contr.* 1990; **112**, 76-82.
[31] OJM Smith. Posicast control of damped oscillatory systems. *Proc. IRE* 1957; **45**, 1249-55.
[32] JY Smith, K Kozak and WE Singhose. Input shaping for a simple nonlinear system. *In*: Proceedings of the American Control Conference, Alaska. 2002, p. 821-6.
[33] Y Sun, M Yang, Y Chen, J Long, J Cao and D Xu. Trajectory error eliminates of input shaping on X-Y platform by Phase Erro feedforward control. *In*: Proceedings of the 22nd International Conference on Electrical Machines and Systems, Harbin, China. 2019.
[34] HD Tho, A Kaneshige and K Terashima. Minimum-time S-curve commands for vibration-free transportation of an overhead crane with actuator limits. *Contr. Eng. Pract.* 2020; **98**, 104390.
[35] DK Thomsen, R Søe-Knudsen, O Balling and X Zhang. Vibration control of industrial robot arms by multi-mode time-varying input shaping. *Mech. Mach. Theor.* 2021; **155**, 104072.
[36] MD Ulriksena, D Bernalb, ME Nielsena and L Damkildea. Damage localization in offshore structures using shaped inputs. *Proc. Eng.* 2017; **199**, 2282-7.
[37] JM Veciana, S Cardona and P Català. Minimizing residual vibrations for non-zero initial states: Application to an emergency stop of a crane. *Int. J. Precis. Eng. Manuf.* 2013; **14**, 1901-8.
[38] A Wahrburg, J Jurvanen, M Niemelä and M Holmberg. Input shaping for non-zero initial conditions and arbitrary input signals with an application to overhead crane control. *In*: Proceedings of the IEEE 17th International Conference on Advanced Motion Control, Padova, Italy. 2022, p. 36-41.
[39] W Wang, C Hu, K Zhou and Z Wang. Time parameter mapping and contour error precompensation for multi-axis input shaping. *IEEE Trans. Ind. Informat.* 2022; **19**, 2640-51.
[40] H Yavuza and S Beller. An intelligent serial connected hybrid control method for gantry cranes. *Mech. Syst. Signal Process.* 2021; **146**, 107011.
[41] HL Zhang, X Lu, DP Jia, BJ Zhao, T Zhang, Y Liu and HY Yan. Position control of XY precision planar motion table based on input shaping filter. *In*: Proceedings of the 2nd International Conference on Electronics, Communications and Information Technology, Sanya, China. 2021, p. 835-9.
[42] W Zhu, Q Zong and B Tian. Adaptive tracking and command shaped vibration control of flexible spacecraft. *IET Contr. Theor. Appl.* 2019; **13**, 1121-8.